Carbohydrate Polymers 83 (2011) 38–43

Contents lists available at ScienceDirect

Carbohydrate Polymers

journal homepage: www.elsevier.com/locate/carbpol

Synthesis and characterization of Ag–Pd alloy nanoparticles/carboxylated cellulose nanocrystals nanocomposites

He Liu[a,b], Dan Wang[a,b], Shibin Shang[a,b], Zhanqian Song[a,b,*]

[a] Institute of Chemical Industry of Forestry Products, Chinese Academy of Forestry (CAF), 16 Suojin Wucun, Nanjing, China
[b] National Engineering Lab for Biomass Chemical Utilization, 16 Suojin Wucun, Nanjing, China

ARTICLE INFO

Article history:
Received 10 June 2010
Received in revised form 30 June 2010
Accepted 7 July 2010
Available online 13 July 2010

Keywords:
Cellulose nanocrystal
Ag–Pd alloy
Nanoparticle
Nanocomposite
DNA hybridization

ABSTRACT

Synthesis of Ag–Pd alloy nanoparticles was carried out with carboxylated cellulose nanocrystals as the scaffolds by reducing metallic cations using $NaBH_4$. Alloy particles with a size less than 10 nm were readily prepared and dispersed well. The average size of alloy nanoparticles decreased as the increasing molar ratio of Ag/Pd. The carboxyl and hydroxyl groups of carboxylated cellulose nanocrystals supplied a coordination effect to adsorb metallic cations and alloy nanoparticles to prevent the aggregation of nanoparticles. The carboxylated cellulose nanocrystals as platforms carrying Ag–Pd alloy nanoparticles were used as labels for electrical detection of DNA hybridization.

1. Introduction

Synthesis and applications of metallic nanoparticles have attracted a lot of attention due to their unique physical and chemical properties, which are greatly affected by size, shape and dispersion stability of particles (Feldheim & Foss, 2001; Rao, Muller, & Cheetham, 2004; Sun & Xia, 2002). Nanoalloys often have excellent properties than monometal and have been utilized in a number of important areas, ranging from catalysis to optoelectronic, magnetic, and medical applications. Recently, biodiagnostics is of special interest and bimetallic nanoalloys have shown to be promising biodiagnostic agents due to their tenability of composition, ordering size, and shape (Ferrando, Jellinek, & Johnston, 2008). Metallic and bimetallic nanoparticles are generally produced by reducing metal salts in the presence of surfactants (e.g., citrate, alkylthiols, or thioethers) or polymeric ligands (e.g., polyvinylpyrrolidone), which passivates the cluster surface (Bönnemann & Richards, 2001; Mallin & Murphy, 2002; Sun & Xia, 2002; Toshima & Yonezawa, 1998). These surfactants and polymeric ligands are made from petrochemicals which are non-renewable. As fossil resources are limited, finding renewable and biodegradable alternative is promising.

Cellulose, as a natural, renewable and biodegradable polymer, is abundant. It is a linear oxygen-rich carbohydrate (polysaccharide) consisting of anhydroglucose units connected by an oxygen linkage. Previous works show porous cellulose fibers can be used as a nanoreactor and cellulose nanocrystals (CNXLs) can act as scaffolds for the synthesis of metallic nanoparticles (Cai, Kimura, Wada, & Kuga, 2009; He, Kunitake, & Nakao, 2003; Shin, Bae, Arey, & Exarhos, 2008). CNXLs can be prepared by the acid hydrolysis from a variety of sources (Cao, Dong, & Li, 2007; Roohani et al., 2008). CNXLs have a good dispersing ability in distilled water and the suspension does not make sediment or flocculate because of the abundant hydroxyl group and a consequence of sulfate groups on the surface of CNXLs created during the sulfuric acid treatment (Dong, Kimura, Revol, & Gray, 1996). In suspension of metallic salts and CNXLs, most metallic cations are absorbed on the surface of CNXLs *via* electrostatic interactions between oxygen atoms of polar hydroxyl and transition metallic cations (He et al., 2003). These effects control the size by preventing the aggregation of metallic particles reduced from metallic cations. So nanoparticles which were synthesized *via* CNXLs may be as small as quantum dots.

Hybrid systems consisting of quantum dots coupled to biomaterials are important in nanobiotechnology (Bruchez, Moronne, Gin, Weiss, & Alivisatos, 1998; Mattoussi et al., 2000). Previous studies indicate that nanoparticles can be used in a variety of bio-analytical formats *via* electrochemical detection. Activated carbon-nanotubes

* Corresponding author at: National Engineering Lab for Biomass Chemical Utilization, 16 Suojin Wucun, Nanjing, China. Tel.: +86 21 85482499; fax: +86 21 85482499.
E-mail addresses: liuheicifp@hotmail.com (H. Liu), wgdan@163.com (D. Wang), shangsb@hotmail.com (S. Shang), songzq@hotmail.com (Z. Song).

0144-8617/$ – see front matter. Crown Copyright © 2010 Published by Elsevier Ltd. All rights reserved.
doi:10.1016/j.carbpol.2010.07.019

were used as platforms to carry more CdS nanoparticles for electrical detection of DNA hybridization (Wang, Liu, Jan, & Zhu, 2003). Numerous applications of cellulose take advantage of its biocompatibility and chirality for the immobilization of proteins (Martinez, Manolache, Gonzalez, Young, & Denes, 2000), antibodies (Loescher, Ruckstuhl, & Seeger, 1998), heparin (Erdtmann, Keller, & Baumann, 1994), DNA (Mangalam, Simonsen, & Benight, 2009), and for the separation of enantiomeric molecules (Goetmar, Zhou, Stanley, & Guiochon, 2004) as well as the formation of cellulose composites with synthetic polymers and biopolymers (Linder, Bergman, Bodin, & Gatenholm, 2003). To the best of our knowledge, using carboxylated CNXLs as platforms for electronic detection of DNA hybridization has not been reported.

In this work, nanocomposites consisting of Ag–Pd alloy nanoparticles loaded on carboxylated CNXLs were prepared and used as oligonucleotide label for the sensitive electrochemical stripping detection of DNA.

2. Experimental

2.1. Materials

2,2,6,6-Tetramethylpiperidine-1-oxyl radical (TEMPO), silver nitrate ($AgNO_3$), palladium chloride ($PdCl_2$), sulfuric acid (H_2SO_4, 98%), sodium borohydride ($NaBH_4$), sodium hypochlorite (NaClO), microcrystalline cellulose, phosphotungstic acid hydrate ($H_3O_{40}PW_{12}{\cdot}H_2O$), sodium bromide (NaBr), sodium hydroxide (NaOH), ammonia ($NH_3{\cdot}H_2O$), cetyltrimethyl ammonium bromide (CTAB), 1-ethyl-3-(3-dimethylaminopropyl) carbodiimide (EDC) and N-hydroxysuccinimide (NHS) were all purchased from Sinopharm Chemical Reagent Co., Ltd. and used as received. 0.2 mol L^{-1} pH 5.4 HAc–NaAc buffer. PBS buffer (8.0 g L^{-1} NaCl–0.2 g L^{-1} KCl–1.44 g L^{-1} Na_2HPO_4–0.2 g L^{-1} KH_2PO_4). 2× SSC buffer (0.3 mol L^{-1} sodium chloride–0.03 mol L^{-1} sodium citrate). 0.2% sodium dodecyl sulfate (SDS). High effect paraffin ceresin. Graphite powder. Solutions were prepared with Aquapro ultrapure water (resistivity: 18 MΩ, Aquaplus AWL-1002-P, Ever Young Enterprises Development Co., Ltd., China).

Materials for the detection of PEP gene sequence: 18-base target DNA sequence (target ssDNA, namely an 18-base fragment of PEP gene sequence, also namely complementary sequence cDNA of DNA probe), and oligonucleotide probe (probe DNA) were purchased from Beijing SBS Gene Technology Limited Company. PEP gene is a promoter of phosphoenolpyruvate carboxylase gene, which is an important promoter in many genetically modified crops. Their base sequences were as below:

Probe DNA: 5′-NH_2-CAG CAC CTA GGC ATA GGT-3′

Target DNA: 5′-ACC TAT GCC TAG GTG CTG-3′

2.2. Preparation and surface modification of cellulose nanocrystal

The suspension of cellulose nanocrystals in water was prepared by acid-catalyzed hydrolysis of microcrystalline cellulose as described (Roohani et al., 2008). The microcrystalline cellulose (6 g) mixed with sulfuric acid solution (90 mL, 64%) and stirred vigorously at 40 °C for 2 h. The suspension was then diluted 10-times and washed repeatedly by diluting with water and centrifuging until the pH of the suspension was about 2. Then dialysis against distilled water was performed to remove free acid in the suspension, as detected by the neutrality of the dialysis effluent. Finally, the CNXLs were dispersed in distilled water and the suspension of CNXLs with a solid content of 1% was obtained through 30 min of ultrasonic treatment.

The modification of cellulose nanocrystal was carried out according to previous references (Goetmar et al., 2004; Saito & Isogai, 2004; Saito, Nishiyama, Putaux, Vignon, & Isogai, 2006). The resulting aqueous CNXLs dispersion was then subjected to oxidation, converting the surface C6 primary hydroxyls to carboxylic acids *via* TEMPO-mediated carboxylation. Briefly, 200 mL of a 1 wt% CNXLs suspension was slowly stirred with 140 mg of TEMPO (70 mg/g CNXLs) and 360 mg of NaBr (180 mg/g CNXLs). An aliquot of 9% NaClO solution was added slowly to the CNXLs suspension, and the pH of the mixture was maintained to be 10.5 at room temperature by adding NaClO solution for 48 h. The reaction was quenched with 30–40 mL of ethanol and then purified by sequentially diluting with filtered deionized water and then concentrating by ultrafiltration until a low, typically 10–20 μS/cm, conductivity was achieved.

2.3. Preparation of metallic nanoparticles/carboxylated CNXLs nanocomposite

Metallic nanoparticles were synthesized in the carboxylated CNXLs suspension with varying the initial Ag/Pd molar ratios (pure Ag, 0.75:0.25, 0.5:0.5, 0.25:0.75, pure Pd). In a typical preparation, different molar fractions of aqueous $AgNO_3$ solution (1.0×10^{-2} M) and aqueous $PdCl_2$ solution (1.0×10^{-2} M, dissolved in 1.5 M aqueous NH_4OH solution) were added to five separated carboxylated CNXLs suspension (30 mL, 1 wt%). For example, $AgNO_3$ (0.5 mL) and $PdCl_2$ (0.5 mL) were added to the carboxylated CNXLs suspension for the 50/50 Ag/Pd alloy system; $AgNO_3$ (0.25 mL) and $PdCl_2$ (0.75 mL) were added for the 25/75 Ag/Pd alloy system. The total molar concentration of cations was constant. After stirring for 1 h, the alloy nanoparticles/carboxylated CNXLs gels were prepared by treating the suspension with an aliquot of $NaBH_4$ (1.0×10^{-2} M) solution at room temperature. The suspension was immediately reduced and was changed from colorless to black. After stirring for another 1 h, the alloy nanoparticles/carboxylated CNXLs nanocomposites were separated in a different phase from suspension by centrifugation at 10,000 rpm.

2.4. Application of metallic nanoparticles/carboxylated CNXLs nanocomposite in DNA detection

Metallic nanoparticles/carboxylated CNXLs nanocomposites homogenous suspension (0.5 mL, 1.0 g L^{-1}) was mixed with probe DNA solution (200 μL, 1.0×10^{-4} M) in PBS solution (pH 7.0) which contained 5.0 mmol L^{-1} EDC, 10.0 mmol L^{-1} NHS and incubated at room temperature for overnight with stirring. The DNA conjugate was then obtained after centrifugating at 10,000 rpm for 30 min, and washing with water and re-centrifugation.

The carbon paste electrode (CPE) was prepared by hand-mixing of graphite powder with paraffin at a ratio of 3/1 (w/w) in a mortar. The homogeneous paste was packed into a cavity of glass tube (Φ = 3.5 mm). The electrical contact was obtained with a copper wire connected to the paste in the tube. The electrode was polished glossily before use. CTAB (1.0×10^{-2} M) was applied onto the CPE surface for 2 h. The electrode was then washed with ultrapure water. A film of CTAB was formed on the surface of CPE, and the modified electrode was denoted as CTAB/CPE.

Target DNA sequence was immobilized on the CTAB/CPE by electrostatic interaction which was performed by dropping target DNA solution onto CTAB modified CPE surface, and the wet electrode was kept at room temperature for remaining 1 h. The resulted target DNA/CTAB/CPE was rinsed by ultrapure water.

Hybridization reaction was carried out by immersing the target DNA/CTAB/CPE into a hybridization solution (in 2× SSC buffer) containing the nanoparticle-labeled DNA probe for 45 min at 40 °C. Then the electrode was washed three times with a 0.2% SDS solution to remove the unhybridized DNA probe and denoted as dsDNA/CTAB/CPE.

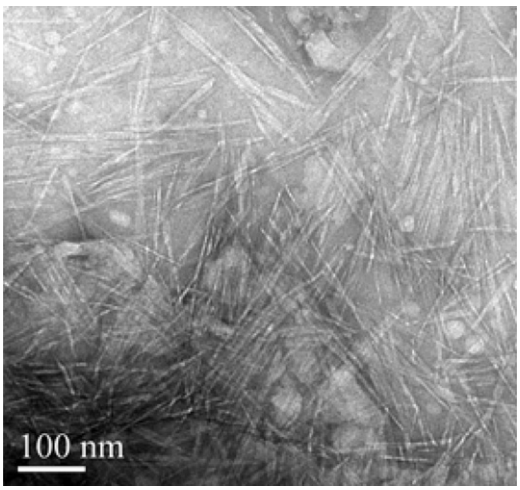

Fig. 1. TEM image of carboxylated CNXLs.

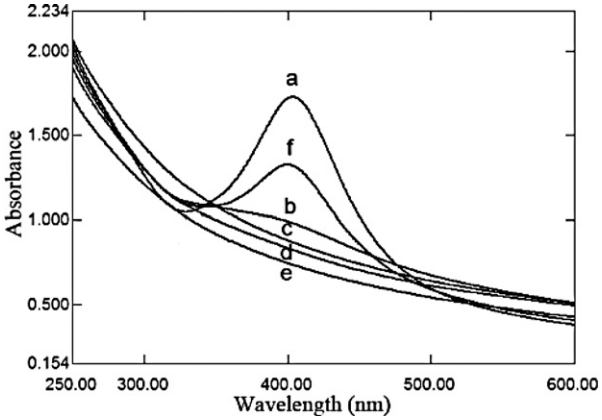

Fig. 2. UV–Vis absorption spectra of alloy nanoparticles and monometallic nanoparticles on carboxylated CNXLs with different molar ratio: (a) 100% Ag, (b) 75% Ag 25% Pd, (c) 50% Ag 50% Pd, (d) 25% Ag 75% Pd, (e) 100% Pd, (f) 50% monometallic Ag 50% monometallic Pd.

After hybridization, the dsDNA/CTAB/CPE was immersed into HNO_3 (100 μL, 1.0 M) for 5 min, and metallic cations were released immediately from the nanoparticles anchored on the hybrids. HAc–NaAc buffer (2.0 mL, pH 5.4), as the supporting electrolyte, was added into above HNO_3 solution. Then a differential pulse anodic stripping voltammetry (DPASV) scan on glassy carbon electrode (GCE) was recorded after an initial electrodeposition for 150 s while stirring. The anodic stripping peak current was determined as the analytical response of DNA biosensor.

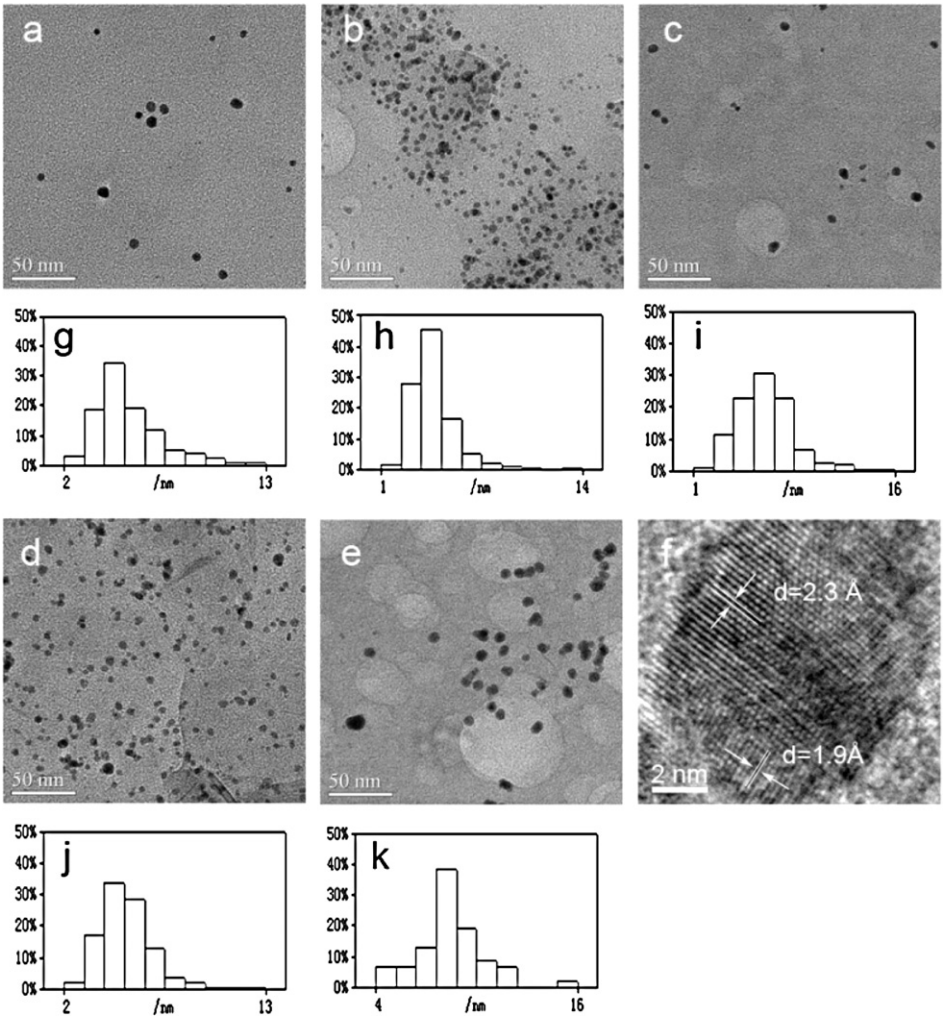

Fig. 3. TEM images and size histograms of Ag–Pd alloy nanoparticles and monometallic nanoparticles: (a,g) 100% Ag, (b,h) 75% Ag 25% Pd, (c,i) 50% Ag 50% Pd, (d,j) 25% Ag 75% Pd, (e,k) 100% Pd, (f) HRTEM image of nanoparticle in Fig. 3(b).

2.5. Characterization

The size and morphology of carboxylated CNXLs and metallic nanoparticles were observed by JEOL transmission electron microscopy (TEM) 2100 microscope. The TEM sample was typically prepared by dropping sample suspension on a Cu grid coated with carbon films, and the TEM images of carboxylated CNXLs were obtained by staining using 1.0% phosphotungstic acid. The high-resolution TEM (HRTEM) image, Scanning Transmission Electron Microscopy (STEM) image and Energy Dispersive X-ray Fluorescence Spectroscopy (EDX) analysis were obtained by FEI Tecnai F20 TEM. Suspensions of monometallic and alloy nanoparticles were characterized using a Shimadzu 2450 UV-Vis spectrophotometer.

A CHI 832 electrochemical analyzer (Shanghai CH Instrument Co., China) with the three-electrode system consisting of the modified carbon paste working electrode, an Ag/AgCl reference electrode, and a platinum wire counter electrode was used. A glassy carbon electrode (GCE) was used for anodic stripping detection of metal.

3. Results and discussion

The TEM image of a dilute suspension of carboxylated CNXLs given in Fig. 1 shows that the suspension contains cellulose fragments consisting of both individual and aggregated nanocrystals. These fragments displayed slender rods with about 10–20 nm in diameter and 100–200 nm in length. The carboxylated CNXLs look bright in the TEM image because of staining obtained by 1.0% phosphotungstic acid.

Carboxylated CNXLs have a strong ability to absorb metallic cations because of abundant carboxyl and hydroxyl groups in carboxylated CNXLs. After treating metallic cations with $NaBH_4$ solution, a different color was observed with different ratios of molar composition of Ag and Pd. The pure Ag on carboxylated CNXLs turned from colorless to light yellow upon reduction. However, as the initial Ag/Pd molar ratios were 0.75:0.25, 0.5:0.5, 0.25:0.75 and pure Pd, colors of suspensions were all black. Five redispersed suspensions of metallic nanoparticles/carboxylated CNXLs complex in distilled water were stable. No obvious deposition or flocculation has been observed in the five suspensions after 4 months.

Fig. 2 shows the UV–Vis spectra of metallic nanoparticles with different initial molar ratios of Ag/Pd. Non-uniform baselines are observed by light scattering of large carboxylated CNXLs rod-like particles. A surface Plasmon resonance band of monometallic Ag nanoparticles at 400 nm and the absence of surface Plasmon resonance band of monometallic Pd from 250 nm to 600 nm are consistent with previous reports (Ferrando et al., 2008; Toshima and Yonezawa, 1998). There was no surface plasmon resonance band of the co-reduction product when the initial Ag/Pd molar ratios were 0.25:0.75 (d), 0.5:0.5 (c) and 0.75:0.25 (b) respectively. An obvious surface plasmon resonance band at 400 nm was observed for monometallic Ag nanoparticles and monometallic Pd nanoparticles mixture (the Ag/Pd molar ratio was 0.5:0.5). In the case of core–shell particles, two peaks detected should be contributed by metals in the core and on the shell (Ferrando et al., 2008). No obvious peak in UV–Vis spectra indicates that the nanoparticles are intermixed and the formation of alloy nanoparticles are homogeneous composition.

TEM images of metallic nanoparticles/carboxylated CNXLs nanocomposites, size histograms of metallic nanoparticles, and HRTEM image of bimetallic nanoparticles are listed in Fig. 3. Images show nanostructures were formed in carboxylated CNXLs suspension. The monometallic nanoparticles and bimetallic nanoparticles

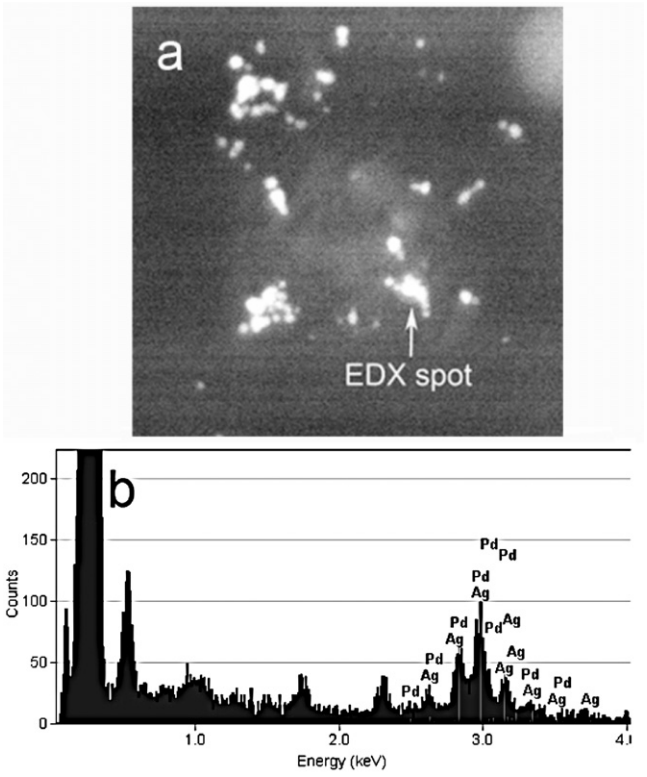

Fig. 4. STEM image (a) and EDX (b) of Ag–Pd alloy nanoparticle.

are dispersed well in the presence of carboxylated CNXLs. Because of strong interactions between the metallic cations and carboxyl or hydroxyl groups on cellulose, metallic cations are uniformly and tightly attached to carboxylated CNXLs. Such interactions would decrease the mobility of metallic cations, prevent the growth of large particles, and stabilize metallic nanoparticles (He et al., 2003; Shinsuke, Manami, Minoru, Hiroyuki, & Hiroyuki, 2009). The characterization gives images of metallic nanoparticles only, because carboxylated CNXLs could not give contrast against the resin (Cai et al., 2009). Sizes of monometallic Ag and Pd nanoparticles are 5.5 ± 3.4 nm and 8.5 ± 4.2 nm (Fig. 3(a) and (e)). And different Ag/Pd molar ratios of 0.75:0.25, 0.5:0.5 and 0.25:0.75 show sizes of 4.3 ± 3.2 nm, 4.9 ± 2.5 nm and 5.3 ± 2.7 nm, respectively (Fig. 3(b), (c) and (d)). It indicates that the average size of alloy nanoparticles decreases as the molar ratio of Ag/Pd increasing. The fact of the dependence of the size of alloy nanoparticles on the composition has been reported by several researchers (Chen & Chen, 2002; Wu, Chen, & Huang, 2001a, 2001b, 2001c; Yonezawa & Toshima, 1995). In addition to the collision energy and the sticking coefficient, rates of nucleation and growth primarily depend on probabilities of collisions between several atoms, between one atom and a nucleus, and between two or more nuclei (Toshima & Yonezawa, 1998). The nucleation is related to the first kind of collisions and the growth process is due to the second and third ones. When the reduction rate was so large that most of ions were reduced before the nucleation, and the probability of effective collisions between one atom and a nucleus was much higher than those of the other two collisions, the size of resultant particles would be monodispersed and determined by the number of the nuclei formed at the very beginning of the reaction (Toshima & Yonezawa, 1998). In this study, the reduction of Ag^+ and Pd^{2+} ions might be so fast that they can be completely reduced before forming nuclei and the sizes of the Ag, Pd and Ag–Pd alloy nanoparticles obtained were determined by the

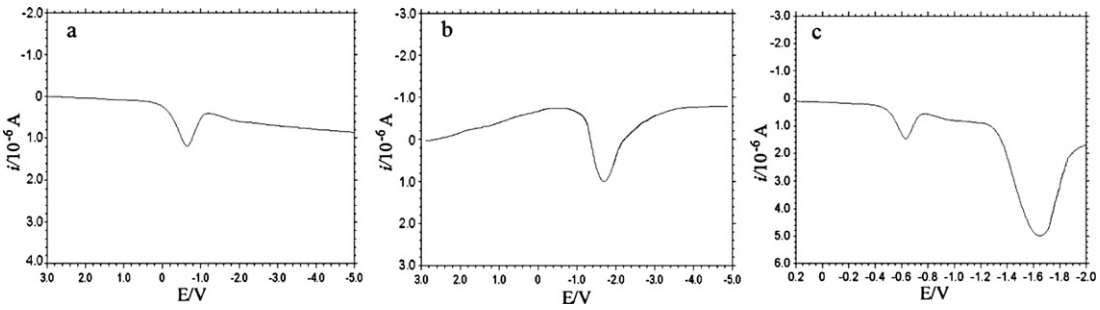

Fig. 5. Differential pulse anodic stripping voltammgrams of the dissolved metal at glassy carbon electrode after: (a) Ag, (b) Pd, (c) Ag–Pd alloy.

number of nuclei formed from Ag or Pd. Since the concentration of total metallic cations was fixed, the significant reduction in size with the addition of Ag implied that Ag might act as the seeds for the formation of Ag–Pd alloy nanoparticles.

The HRTEM image (Fig. 3(f)) of alloy nanoparticles (Ag/Pd molar ratio of 0.75:0.25) indicates the lattice planes with the basal spacing of 2.3 Å and 1.9 Å. It implies that particles must be an alloy and they consist of a homogeneous material. The HRTEM image shows excellent atomic alignment within particles, and there is no lattice distortion which indicates a good mixing of the atomic level of Ag and Pd. The sample is also examined using EDX to determine the composition of individual particle. Fig. 4(a) is a STEM image of as-prepared sample (Ag/Pd molar ratio of 0.75:0.25) and Fig. 4(b) displays the result of EDX analysis of the single particle shown in Fig. 4(a). The EDX analysis indicates that the individual particle is composed of silver and palladium.

Grafting of the probe DNA onto the carboxylated CNXLs was carried out *via* carboxyl groups covalently coupled with the 5′-NH_2 moiety of the probe sequence by amide linkage (–CONH–) in the presence of EDC and NHS (Erdtmann et al., 1994; Huang, Zhou, & Deng, 2000). Target DNA sequence was determined by using nanocomposites labeled DNA probe with DPASV. The DPASV diagrams are shown in Fig. 5. Curve a was the stripping voltammogram of Ag with the detection of target DNA, which had the stripping signal at −0.65 V. Curve b was the stripping voltammogram of Pd with the detection of target DNA, showing a well-defined oxidation peak at −1.6 V. Curve c was the stripping voltammogram of sample Ag–Pd alloy (50% Ag 50% Pd) with the detection of target DNA. The two oxidation peaks of Ag–Pd alloy are at −0.65 V and −1.6 V in curve c, in consistent with monometallic Ag and monometallic Pd, respectively. Both of Ag and Pd signals can reflect the concentration of target DNA. These results indicate that the use of carboxylated CNXLs to link metallic nanoparticles and probe DNA as oligonucleotide labels for the sensitive electrochemical stripping detection of target DNA was feasible.The sensitivity and selectivity of this electrode for tested DNA using carboxylated CNXLs as linkage for the DNA and nanoparticles will be shown in another paper.

4. Conclusion

The as-prepared carboxylated CNXLs as scaffolds for nucleation and growth have been used for the generation of Ag–Pd alloy nanoparticles. The characterization apparently indicates that the prepared bimetallic nanoparticles are alloy with a narrow distribution of particle size. HRTEM image shows the uniform contrast through alloy nanoparticles indicating a good mixing of Ag and Pd. The average size of alloy nanoparticles decreases as the molar ratio of Ag/Pd increases. The DPASV of silver and palladium from Ag–Pd alloy indicates that the Ag–Pd alloy/carboxylated CNXLs nanocomposites can be employed for electrical detection of DNA hybridization.

Acknowledgments

This work was supported by the special research fund of Chinese Academy of Forestry (CAFYBB2007030), and a grant from the National High Technology Research and Development Program of China (863 Program) (No. 2007AA10074)

References

Bönnemann, H., & Richards, R. M. (2001). Nanoscopic metal particles—synthetic methods and potential applications. *European Journal of Inorganic Chemistry*, *10*, 2455–2480.

Bruchez, M., Moronne, M., Gin, P., Weiss, S., & Alivisatos, A. P. (1998). Semiconductor nanocrystals as fluorescent biological labels. *Science*, *281*, 2013–2016.

Cai, S., Kimura, J., Wada, M., & Kuga, S. (2009). Nanoporous cellulose as metal nanoparticles support. *Biomacromolecules*, *10*, 87–94.

Cao, X. D., Dong, H., & Li, C. M. (2007). New nanocomposite materials reinforced with flax cellulose nanocrystals in waterborne polyurethane. *Biomacromolecules*, *23*, 899–904.

Chen, D. H., & Chen, C. J. (2002). Formation and characterization of Au–Ag bimetallic nanoparticles in water-in-oil microemulsions. *Journal of Materials Chemistry*, *12*, 1557–1562.

Dong, X. M., Kimura, T., Revol, J. F., & Gray, D. G. (1996). Effects of ionic strength on the isotropic-chiral nematic phase transition of suspensions of cellulose crystallites. *Langmuir*, *12*, 2076–2082.

Erdtmann, M., Keller, R., & Baumann, H. (1994). Photochemical immobilization of heparin, dermatan sulphate, dextran sulphate and endothelial cell surface heparan sulphate onto cellulose membranes for the preparation of athrombogenic and antithrombogenic polymers. *Biomaterials*, *15*, 1043–1048.

Feldheim, D. L., & Foss, C. A. (2001). *Metal nanoparticles synthesis, characterization and applications*. New York: Marcel Dekker, Inc.

Ferrando, R., Jellinek, J., & Johnston, R. L. (2008). Nanoalloys: From theory to applications of alloy clusters and nanoparticles. *Chemical Reviews*, *108*, 845–910.

Goetmar, G., Zhou, D., Stanley, B. J., & Guiochon, G. (2004). Heterogeneous adsorption of 1-indanol on cellulose tribenzoate and adsorption energy distribution of the two enantiomers. *Analytical Chemistry*, *76*, 197–202.

He, J. H., Kunitake, T., & Nakao, A. (2003). Facile in situ synthesis of noble metal nanoparticles in porous cellulose fibers. *Chemistry of Materials*, *15*, 4401–4406.

Huang, E., Zhou, F. M., & Deng, L. (2000). Studies of surface coverage and orientation of DNA molecules immobilized onto preformed alkanethiol self-assembled monolayers. *Langmuir*, *16*, 3272–3280.

Linder, A. P., Bergman, R., Bodin, A., & Gatenholm, P. (2003). Mechanism of assembly of xylan onto cellulose surfaces. *Langmuir*, *19*, 5072–5077.

Loescher, F., Ruckstuhl, T., & Seeger, S. (1998). Ultrathin cellulose-based layers for detection of single antigen molecules. *Advanced Materials*, *10*, 1005–1009.

Mallin, M. P., & Murphy, C. J. (2002). Solution-phase synthesis of sub-10 nm Au–Ag alloy nanoparticles. *Nano Letters*, *2*, 1235–1237.

Mangalam, A. P., Simonsen, J., & Benight, A. S. (2009). Cellulose/DNA hybrid nanomaterials. *Biomacromolecules*, *10*, 497–504.

Martinez, A. J., Manolache, S., González, V., Young, R. A., & Denes, F. (2000). Immobilized biomolecules on plasma functionalized cellophane. I. Covalently attached alpha-chymotrypsin. *Journal of Biomaterials Science, Polymer Edition*, *11*, 415–438.

Mattoussi, H., Mauro, J. M., Goldman, E. R., Anderson, G. P., Sundar, V. C., Mikulec, F. V., et al. (2000). Self-assembly of CdSe–ZnS quantum dot bioconjugates using an engineered recombinant protein. *Journal of the American Chemical Society*, *122*, 12142–12150.

Rao, C. N. R., Muller, A., & Cheetham, A. K. (2004). *The chemistry of nanomaterials: Synthesis, properties and applications*. Weinheim: Wiley-VCH Verlag Gmbh & Co. KGaA.

Roohani, M., Habibi, Y., Belgacem, N. M., Ebrahim, G., Karimi, A. N., & Dufresne, A. (2008). Cellulose whiskers reinforced polyvinyl alcohol copolymers nanocomposites. *European Polymer Journal*, *44*, 2489–2498.

Saito, T., & Isogai, A. (2004). TEMPO-mediated oxidation of native cellulose. The effect of oxidation conditions on chemical and crystal structures of the water-insoluble fractions. *Biomacromolecules*, *5*, 1983–1989.

Saito, T., Nishiyama, Y., Putaux, J. L., Vignon, M., & Isogai, A. (2006). Homogeneous suspensions of individualized microfibrils from TEMPO-catalyzed oxidation of native cellulose. *Biomacromolecules*, *7*, 1687–1691.

Shin, Y., Bae, I., Arey, B. W., & Exarhos, G. J. (2008). Facile stabilization of gold–silver alloy nanoparticles on cellulose nanocrystal. *The Journal of Physical Chemistry C*, *112*, 4844–4848.

Shinsuke, I., Manami, T., Minoru, M., Hiroyuki, S., & Hiroyuki, Y. (2009). Synthesis of silver nanoparticles templated by TEMPO-mediated oxidized bacterial cellulose nanofibers. *Biomacromolecules*, *10*, 2714–2717.

Sun, Y. G., & Xia, Y. N. (2002). Shape-controlled synthesis of gold and silver nanoparticles. *Science*, *298*, 2176–2179.

Toshima, N., & Yonezawa, T. (1998). Bimetallic nanoparticles-novel materials for chemical and physical applications. *New Journal of Chemistry*, *22*, 1179–1201.

Wang, J., Liu, G. D., Jan, M. R., & Zhu, Q. Y. (2003). Electrochemical detection of DNA hybridization based on carbon-nanotubes loaded with CdS tags. *Electrochemistry Communications*, *5*, 1000–1004.

Wu, M. L., Chen, D. H., & Huang, T. C. (2001a). Preparation of Au/Pt bimetallic nanoparticles in water-in-oil microemulsions. *Chemistry of Materials*, *13*, 599–606.

Wu, M. L., Chen, D. H., & Huang, T. C. (2001b). Synthesis of Au/Pd bimetallic nanoparticles in reverse micelles. *Langmuir*, *17*, 3877–3883.

Wu, M. L., Chen, D. H., & Huang, T. C. (2001c). Preparation of Pd/Pt bimetallic nanoparticles in water/aot/isooctane microemulsions. *Journal of Colloid and Interface Science*, *243*, 102–108.

Yonezawa, T., & Toshima, N. (1995). Mechanistic consideration of formation of polymer-protected nanoscopic bimetallic clusters. *Journal of the Chemical Society, Faraday Transactions*, *91*, 4111–4119.